Free Radical Research, August 2010; 44(8): 843–853

informa
healthcare

The synthetic polyphenol *tert*-butyl-bisphenol inhibits myoglobin-induced dysfunction in cultured kidney epithelial cells

ANU SHANU[1,2], SARAH N. PARRY[1], SARAH WOOD[1,2], ELICIA RODAS[2] & PAUL K. WITTING[1,2]

[1]*Discipline of Pathology, Redox Biology Group, The University of Sydney, Sydney, NSW, 2006, Australia, and*
[2]*Vascular Biology Group, ANZAC Research Institute, Concord Repatriation General Hospital, Concord NSW 2139, Australia*

(Received date: 19 January 2010; In revised from date: 8 April 2010)

Abstract
Rhabdomyolysis caused by severe burn releases extracellular myoglobin (Mb) that accumulates in the kidney and urine (maximum [Mb] ~ 50 μM) (termed myoglobinuria). Extracellular Mb can be a pro-oxidant. This study cultured Madin-Darby-canine-kidney-Type-II (MDCK II) cells in the presence of Mb and tested whether supplementation with a synthetic *tert*-butyl-polyphenol (*tert*-butyl-bisphenol; *t*-BP) protects these renal cells from dysfunction. In the absence of *t*-BP, cells exposed to 0–100 μM Mb for 24 h showed a dose-dependent decrease in ATP and the total thiol (TSH) redox status without loss of viability. Gene expression of superoxide dismutases-1/2, haemoxygenase-1 and tumour necrosis factor increased and receptor-mediated endocytosis of transferrin and monolayer permeability decreased significantly. Supplementation with *t*-BP before Mb-insult maintained ATP and the TSH redox status, diminished antioxidant/pro-inflammatory gene responses, enhanced monolayer permissiveness and restored transferrin uptake. Overall, bolstering the total antioxidant capacity of the kidney may protect against oxidative stress induced by experimental myoglobinuria.

Keywords: *Antioxidant, oxidative stress, myoglobinuria, burns, polyphenol, acute renal failure*

Introduction

Acute renal failure (ARF) is a clinical manifestation of severe burn—its incidence varies between 1–39% of patients [1,2]. This low-frequency observed clinically is, however, offset by a high mortality rate, ~ 85% [3,4]. One factor affecting kidney function in burns patients is burn thickness—full thickness burns penetrate tissue, damaging muscle or bone, which can lead to secondary tissue necrosis and the release of toxic factors (e.g. myoglobin (Mb)) into the blood [5,6] in a process termed myoglobinuria.

A significant body of evidence indicates that pro-oxidant Mb accumulates in the kidney during myoglobinuria [7–9]. Myoglobin accumulation within the nephron promotes vasoconstriction and tubular obstruction—a decrease in renal perfusion is consistently reported in animal models of myoglobinuria [10,11]. Pro-oxidant Mb reacts with peroxides to generate reactive oxygen species that can damage a wide range of biomolecules [12,13]. Detection of urinary cross-linked Mb formed upon reaction of the protein and peroxides supports the argument that the kidney is exposed to increased oxidative stress during myoglobinuria [13]. However, adjunctive therapies aimed at inhibiting oxidative damage to the kidney are not routinely employed in the clinical management of burns.

Myoglobin-stimulated vasoconstriction is caused by multiple mechanisms that involve the dysregulation of nitric oxide ($^{\bullet}$NO) homeostasis. For example, formation of a stable haem-NO complex (K_d ~ 10^{-5} M) and, at least in the case of human Mb, a stable *S*-nitrosothiol [14] can affect $^{\bullet}$NO-bioavailability. In addition, oxygenated-Mb rapidly

Correspondence: Dr Paul K. Witting, Discipline of Pathology, Bosch Research Institute, The University of Sydney, NSW, 2006 Australia. Tel: 61-2-9114-0524. Fax: 61-2-9351-2429. Email: pwitting@med.usyd.edu.au

ISSN 1071-5762 print/ISSN 1029-2470 online © 2010 Informa UK Ltd.
DOI: 10.3109/10715762.2010.485993

oxidizes ($k \sim 10^{-6}$–10^{-7} $M^{-1}s^{-1}$) $^{\bullet}NO$ to NO_3^- to yield ferric Mb in this process [15]. Alternatively, Mb can induce lipid oxidation [16] and these oxidized lipids can affect vascular tone. Finally, Mb-oxidants promote endothelial cell apoptosis, which may be relevant to vascular dysfunction [17]. Together, these factors decrease the $^{\bullet}NO$ bioavailability and compound the effects of renal dysfunction [7,18].

We recently demonstrated that low concentrations of extracellular Mb can promote kidney epithelial cell dysfunction through a mechanism of enhanced oxidative stress, as judged by decreases in the total thiol (TSH) redox ratio and an increase in early antioxidant response genes, e.g. superoxide dismutase 1/2 (superoxide dismutase 1-(CuZnSOD) and 2-(MnSOD), catalase (CAT) and haemoxygenase-1 (HO-1), in the absence of any measurable change in cell viability [19]. Oxidative stress and inflammatory responses are closely related [20] in patients with ARF. Several studies have indicated inflammation follows oxidative stress by induction of redox-sensitive Nuclear Factor Kappa Beta (NF-κB) [21]. Furthermore, myoglobin can induce NF-κB activation leading to up-regulation of genes including Tumour Necrosis Factor α (TNFα) [21] and vascular adhesion molecules [22]. Taken together, these data support the idea that bolstering the cellular antioxidant capacity may protect kidney epithelial cells from Mb-induced damage.

Materials and methods

Materials

Chemicals were of the highest quality available. The polyphenol *3,3',5,5'-tetra-t-butyl-biphenyl-4,4'-diol* (referred to here as *t*-BP) was obtained from Maybridge (Cornwall, UK). Cell culture materials were from Sigma (Australia). Buffers were prepared with MilliQ® Water.

Cell culture

Kidney epithelial cells (MDCK II, ATCC, VA) were cultured as described previously [19]. Where required, cells were harvested with 0.1% v/v trypsin and cell pellets isolated by centrifugation (358 × *g*, 4°C).

Pre-treatment of MDCK II cells with t-BP

Plates of cells were randomly allocated for control or *t*-BP pre-treatment. Cells were washed twice in phosphate buffer (PBS; 50 mM, pH 7.4) and treated with vehicle (control) or 10, 50 or 100 μM *t*-BP diluted in HEPES-buffered physiologic salt solution (HPSS; 22 mM HEPES (pH 7.4), 124 mM NaCl, 5 mM KCl, 1 mM $MgCl_2$, 1.5 mM $CaCl_2$, 0.16 mM HPO_4, 5 mM $NaHCO_3$ and 5.6 mM D-glucose). After 2 h at 37°C, cells were washed then treated with Mb or vehicle (control). The *t*-BP concentrations employed in this study reflect plasma levels in rabbits and mice supplemented with dietary *t*-BP (0.2% w/w) for 12 weeks [23,24].

Cell model of myoglobinuria

Equine heart Ferric myoglobin (Sigma-Aldrich, Sydney, Australia) was used to establish the cell model of myoglobinuria. Myoglobin solutions were freshly prepared in PBS, filtered through 0.2 μm pore-size filters to sterilise (Millipore, Australia) and standardised using ε_{409nm} = 188 $mM^{-1}cm^{-1}$ [12]. All solutions prepared in this way displayed a major absorbance at 409 nm assigned as ferric haem with no other absorbance in the range 410–425 nm indicative of the absence of ferrous-oxy-Mb. Myoglobin samples were then diluted in culture medium to final concentrations of 0–100 μM for use in cell studies. After 24 h re-culture, cells were washed (PBS) and harvested for assays outlined below.

Cell viability

Apoptosis and necrosis. Flow cytometry (FACScan, BD, San Diego, CA) was used to assess cell death in Mb- or vehicle-treated (control) cells as described previously [25,26]. Apoptosis and necrosis were expressed as a percentage of annexin V or propidium iodide-positive cells in the total cell population.

Caspase-3/7-activation. A Caspase-Glo™ kit (Promega, Australia) was used to assess caspase activity in MDCK-II cells in the absence (control) or presence of added Mb as per manufacturer's instructions. Luminescence was measured using a Victor III Multi-label plate reader (Perkin Elmer). Activity data were normalised against corresponding protein content (see below) and expressed as fold-change compared to the control.

Cellular ATP levels

Intracellular ATP was determined in Mb- and vehicle-treated (control) cells with an ATPlite® kit as described previously [25]. Luminescence was measured using a Victor III plate reader, normalised for corresponding protein content and expressed in units of nmol/mg cell protein.

Assessment of cellular glutathione redox status

Total thiol (TSH) and its corresponding oxidised disulphide product (TSST) were determined in

cultured MDCK II cells as follows. Cell pellets were resuspended in complete buffer (50 mM phosphate buffer (pH 7.4), 1 mM EDTA, 10 μM butylated hydroxytoluene (Sigma, Australia) and protease inhibitor cocktail (Roche, Mannheim, Germany)) and divided into two equal samples. Each sample was lysed with three cycles of freeze–thaw, centrifuged (5000 × *g*) and the supernatants collected for analysis. One sample was assessed immediately for TSH content by incubating with 62.5 μM 5, 5'-dithiobis(2-nitrobenzoic acid) (Sigma, Australia) at 37°C for 10 min and measuring absorbance at 420 nm. The matched sample was incubated at 37°C with 10 units/mL glutathione reductase and 100 μM NADPH to reduce TSST disulphide to TSH. After 1 h, the samples were treated with 62.5 μM 5,5'-dithiobis(2-nitrobenzoic acid) and absorbance re-determined. TSH concentration was calculated by comparison with a standard curve generated with authentic TSH (Sigma, Australia). Total TSH was normalised to cell protein, while levels of TSST were calculated as the difference between protein-normalised values of TSH in the matched samples. Absorbance spectroscopy was performed with a multi-label Victor III plate reader.

Antioxidant gene regulation

Reverse transcription and RT-PCR. MDCK II cells were lysed and total RNA extracted with a commercial kit (GenElute, Sigma, Australia). Complementary DNA was constructed and gene regulation was assessed initially with RT-PCR using an Eppendorf Mastercycler as described previously [27]. Primers and annealing temperatures are listed in Table I. Products were photographed under UV light and images transformed to tagged-image-files for manipulation with Microsoft Power-point (2000). Densitometry was performed with ImageJ v1.28 software (http://rsh.info.nih.gov//ij/, NIH, USA) and data expressed as fold-change in *β*-actin-normalised gene expression.

qRT-PCR. Where required a Corbett Rotor Gene 6000 was used to perform quantitative PCR. cDNA samples (1 μL) were mixed with SYBR GreenER Master Mix (Invitrogen, 12.5 μL), appropriate primers (final concentration 400 nM; see Table I) and RNAse-free water (9.5 μL). Cycling was as follows: activation (95°C, 8.5 min), 45 cycles of initiation (95°C, 15 s), annealing and elongation (60°C, 1 min), followed by a melt-step (55–95°C). Relative gene expression was assessed using the comparative *Ct* (Δ*Ct*) method and normalised to *β*-actin.

SOD activity

Total SOD activity was assessed by measuring inhibition of pyrogallol (Sigma, Australia) auto-oxidation at 405 nm over 30 min as described [28]. Total SOD activity was expressed as a protein-normalised fold-change in rate relative to the control.

Evaluation of monolayer permeability

Cells were seeded (1×10^5 cells/mL) onto 6-well, 0.4 μm pore size, transparent transwells (ThinCerts Greiner, Germany) and cultured to 90% confluence. Following pre-treatment with *t*-BP or vehicle alone (as control), cells were exposed to 0, 5, 25 and 100 μM Mb. After 24 h, cells were treated with 2.5 μCi of [^{3}H]-inulin/mL complete media (Sigma, Australia) and the [^{3}H]-label assayed with a scintillation counter (Packard-Bell, CA) as described previously [19,29].

Endocytosis of fluorescent transferrin

Preparations of MDCK II cells were supplemented with 100 μM *t*-BP or vehicle alone (control) and then exposed to Mb or vehicle, as indicated in the figure legends. After 24 h, the cells were harvested and pellets of Mb-treated and untreated (control) cells were resuspended in 1 mL of PBS and treated with transferrin conjugated to Alexofluor 488 (5 μg/mL; Invitrogen, Australia) and analysed with flow cytometry [19].

Table I. Forward and reverse primer sequences for use in gene analyses studies.[a]

Gene	Sense	Anti-sense	Annealing temperature (°C)
β-actin	5′-AGCCATGTACGTAGCCATCC-3′	5′-CTCTCAGCTGTGGTGGTGAA-3′	60
SOD-1	5′-TCCACGTCCATCAGTTTGAA-3′	5′-GTCACCTTTGCCCAAGTCAT-3′	60
SOD-2	5′-GGGTTGGCTTGGTTTCAATA-3′	5′-TGCAAGCCATGTATCTCTCG-3′	60
HO-1	5′-GCGTCGACTTCTTCACCTTC-3′	5′-GGTCCTCAGTGTCCTTGCTC-3′	60
TNF*α*	5′-GAGCCGACGTGCCAATG-3′	5′-CAACCCATCTGACGGCACTA-3′	60
NF-*κ*B	5′-AACCCGTAGTGTCAGATGCC-3′	5′-GGACGAACACAGAGGTTGGT-3′	60
VCAM	5′-CAACTGAGTGGCCCCCTAG-3′	5′-GAGATCATTGCCATTCAGCA-3′	60
ICAM	5′-AGAGAGGCTGCACTCCACAG-3′	5′-GCTCACTCAGGGTCAGGTTG-3′	60

[a]Primers were from Sigma-Proologo (Lismore, Australia) and diluted to 10 μM before use.

Protein analysis

Protein concentrations were determined using the bicinchoninic acid assay (Sigma, Australia). Values were used to account for differences in cell density.

Octanol–water partition coefficients

Where required, partitioning of the phenolic compounds (Table II) was determined by assessing the distribution of the pure phenol between octanol and water at 220 nm at 20°C, as described previously [30].

Statistical analyses

Statistical analyses were performed with Prism (GraphPad, San Diego, CA). Data are presented as mean ± SD of replicate analyses from three or five independent experiments (as indicated). Differences between paired data sets were assessed with one-way ANOVA using Bonferroni's multiple comparisons. Significance was accepted at the 95% level; $p < 0.05$.

Results

The synthetic antioxidant t-BP

The redox potential (Table II) measured for *t*-BP is less positive than that for other common synthetic or natural phenols (e.g. probucol and *α*-tocopherol—the most biologically active vitamin E isoform) and is indicative of increased antioxidant activity *in vitro* [31]. Overall, decreasing the redox potential in the design of *t*-BP was achieved without marked alteration of the octanol–water partition coefficient (Table II).

Cell viability in Mb-treated kidney epithelial cells

Consistent with our previous data [19], exposure of cultured MDCK II cells to extracellular Mb did not affect cell viability (Figure 1A . The extents of apoptosis (range 3.1–4.0%), and necrosis (range 4.7–6.6%) were not different to the controls—the level of cell death remained below 11% across all Mb doses tested. Furthermore, activation of the caspases-3/7 (a surrogate marker for early stage apoptosis) remained at near baseline levels in response to added Mb at least when measured 24 h after the insult (Figure 1B). These data suggest ~ 90% of epithelial cells exposed to 0–100 μM Mb remained viable and, therefore, the impact of Mb on molecular/biochemical homeostasis is independent of cytotoxicity.

Cellular ATP in cultured MDCK II cells

Levels of intracellular ATP were measured as an indicator of the balance between energy consumption and production (Figure 2A). In the absence of *t*-BP, Mb induced a significant decrease in ATP, with levels falling from 5.8 nmol/mg cell protein in control cells to 2.6 nmol/mg cell protein in cells exposed to the highest dose of Mb.

Evaluation of cellular total thiol redox status

Monitoring the TSH redox status (defined as the ratio [TSH]/[TSST + TSH]) is an effective means for assessing oxidative stress in cells and tissues [32]. In the absence of *t*-BP, exposure of the cells to extracellular Mb elicited a dose-dependent trend to decrease the TSH redox ratio (Figure 2B) that reached significance for cells exposed to 25 and 100 μM Mb.

Table II. Redox potentials and octanol–water partition coefficients for natural and synthetic phenolic compounds.[a]

Agent	Structure	One-electron potential (mV)	Partitioncoefficient[b]
Probucol	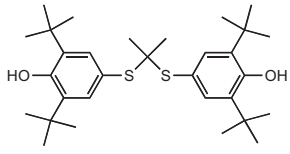	545	12.1
t-BP	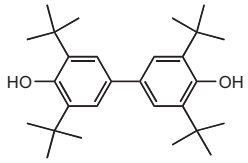	307	10.3
Vitamin E(*α*-TOH)	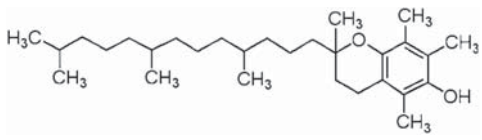	480	12.2

[a]Where required, redox potentials were determined with cyclic volatammetry as described previously [59].
[b]Octanol–water partition coefficients for each sample were determined as described in the Materials and methods section.

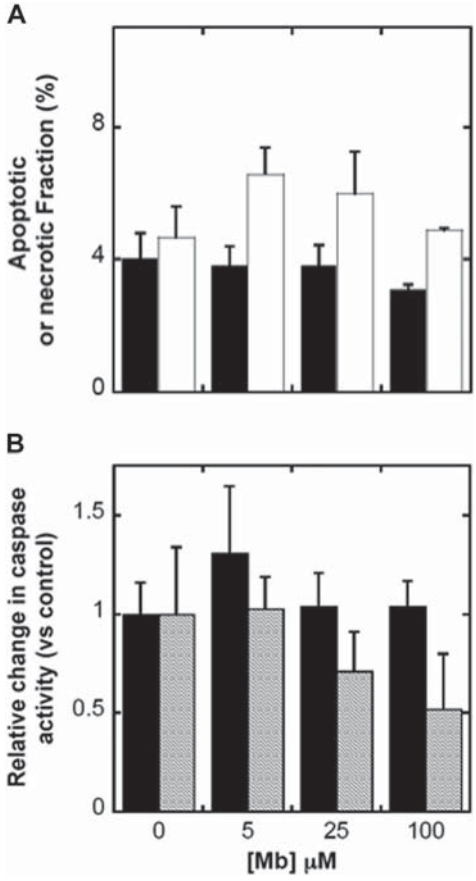

Figure 1. Confluent MDCK II cells were cultured with 0 (*control*), 5, 25 or 100 μM Mb for 24 h and cell viability analysed as (A) apoptosis (*black bar*) or necrosis (*white bar*) in response to Mb-treatment (maximum levels 4 ± 0.8 (0 μM) and 6.6 ± 0.8 (5 μM Mb) %, respectively). (B) Protein-normalized activation of effector caspases-3/7 in the presence of increasing [Mb] with (*hatched bar*) and without (*black bar*) 100 μM *t*-BP pre-treatment. Data represent mean ± SD, $n = 6$ experiments.

Together these data support the idea that extracellular Mb induces a heightened state of oxidative stress in kidney epithelial cells.

Gene regulation in MDCK II treated with Mb

Regulation of the antioxidant response enzymes *SOD-1*, *SOD-2* and *HO-1* was assessed by RT-PCR and normalised to *β-actin* (Figure 3A), with the corresponding histograms shown for *SOD-2* (Figure 3B) and *HO-1* (Figure 3C). Consistent with Mb eliciting a heightened oxidative stress, genes encoding for *SOD-2* and *HO-1* increased in response to Mb insult, with expression reaching ~ 2- and 4-fold higher than the control, respectively. Similarly, the gene encoding for *SOD-1* increased ~ 3-fold (not shown), indicating that MDCK II cells respond to Mb by increasing cytoplasmic and mitochondrial capacity to dismutate $O_2^{\bullet-}$ as well as potentially enhancing haem catabolism. The gene response for

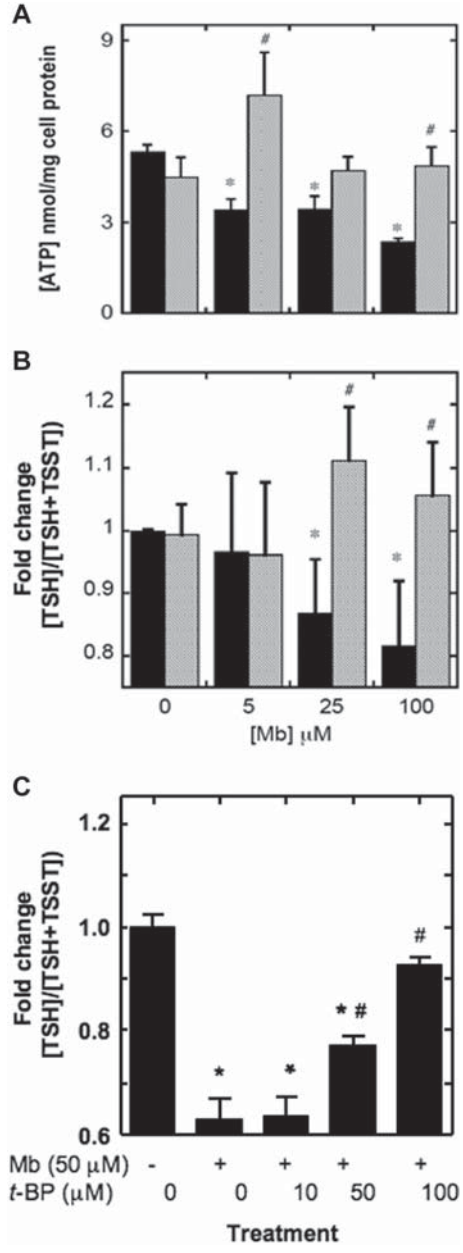

Figure 2. Confluent MDCK II cells were treated in the absence (*control*) or presence of 100 μM *t*-BP and subsequently exposed to Mb (*doses shown*) for 24 h and (A) ATP assessed in the absence (*black bars*) or presence (*hatched bars*) of *t*-BP. (B) The total thiol redox ratio ([TSH]/[TSST+TSH]) in the absence (*black bars*) or presence of *t*-BP (*hatched bars*). Panel (C) shows the [TSH]/[TSST+TSH] ratio in cells pre-treated with *t*-BP (10–100 μM), then 50 μM Mb. Data represent mean ± SD, $n = 6$ (A or B) or 4 (C) experiments. *Significantly different to the control; $p < 0.05$. #Significantly different to the corresponding Mb-treated group; $p < 0.05$.

HO-1 and *SOD-2* were verified by quantitative PCR (Table III). Extracellular Mb also up-regulated the expression of pro-inflammatory TNF*α* and Vascular Cell Adhesion Molecule (VCAM) in MDCK II cells (Table III). In contrast, NF-κB and Intercellular Adhesion Molecule (ICAM) showed no significant changes (Table III).

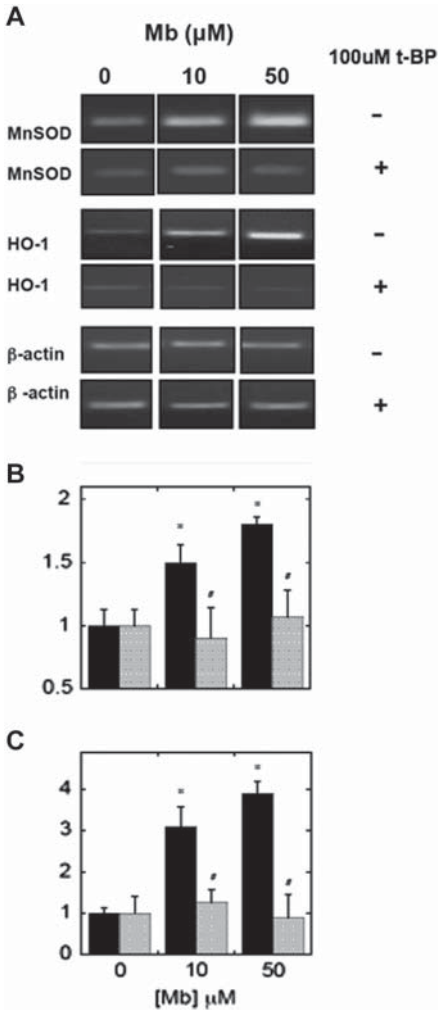

Figure 3. Analysis of *SOD-2* and *HO-1* gene regulation in MDCK II cells exposed to Mb. Confluent MDCK II cells were treated with Mb in the absence (*control*) or presence of 100 μM *t*-BP pre-treatment. After 24 h, cells were harvested and probed for antioxidant gene expression. Panel (A) shows representative Mb dose-dependent gene expression for *SOD-2* and *HO-1* normalised to the corresponding *β-actin* in the absence and presence of 100 μM *t*-BP. Histograms (B) and (C) show the fold-changes in *SOD-2* and *HO-1*, respectively, in the absence (*black bars*) and presence (*hatched bars*) of *t*-BP, at different Mb dose. Data represent mean ± SD from $n = 5$ different cell preparations. *Significantly different to the control; $p < 0.05$. #Significantly different to the corresponding Mb Mb-treated group; $p < 0.05$.

Total SOD activity in Mb-treated MDCK II cells

In the absence of *t*-BP, treatment of confluent MDCK II cells with extracellular Mb elicited a marginal and dose-dependent increase in the inhibition of pyrogallol autoxidation up to 1.2 ± 0.1-fold, which, although modest, was statistically significant (Figure 4). These data are consistent with the enhanced expression of *SOD-1/2* observed at the gene level leading to production of the corresponding active protein(s) (Figure 3).

Assessment of monolayer permeability

Monitoring the transport of [^{3}H] inulin across confluent cells provided an indication of the bulk monolayer integrity for Mb-treated MDCK II cells [33,34]. Permeability of the epithelial monolayer decreased dose-dependently with Mb challenge (Figure 5A). The decline in permeability reached significance at 25 and 100 μM Mb, where monolayer permissiveness decreased up to 20% compared to the control.

Receptor-mediated endocytosis of transferrin in cultured MDCK II cells

Receptor-mediated endocytosis of fluorescently-labelled transferrin was quantified by flow cytometry. A representative scatter plot from vehicle-treated (control) cells is shown in Figure 6A, and the corresponding histogram shown in Figure 6B. The presence of two populations was indicative of two distinct intracellular pools of transferrin. The two pools of transferrin were assigned previously as a slow-cycling population of transferrin-receptor complex that is mobilized to the Golgi apparatus and, a pool of fast-cycling transferrin-receptor complex that releases transferrin in the cytoplasm and returns to the plasma membrane without translocating to the Golgi [35]. In response to Mb insult, the leftmost peak was largely unaffected whereas the rightmost peak decreased in cells exposed to 100 μM Mb (Figure 6C). Quantitative analysis (accounting for both peak responses) showed a progressive Mb-dependent loss in mean fluorescence intensity, reaching 65% inhibition of receptor-mediated endocytosis at the highest dose of Mb (Figure 7).

Supplementation of cultured kidney epithelial cells with added t-BP

Supplementation with *t*-BP resulted in overall enhanced cell function, as judged by a number of parameters. Thus, caspase-3/7-activity decreased marginally (Figure 1B) and intracellular ATP increased (Figure 2A), indicating improved viability. Added to this, the TSH redox ratio showed a dose-dependent increase in cells pre-treated with *t*-BP, with 100 μM *t*-BP completely reversing the effect of added Mb (Figure 2C). These data imply that the heightened state of oxidative stress induced by Mb was inhibited through antioxidant supplementation. Furthermore, the gene expression of *SOD-2*, *HO-1*, *TNFα* and Vascular cell adhesion molecule (*VCAM*) genes remained at basal levels in cells pre-treated with 50 and 100 μM, indicating that the ≥ 50 μM *t*-BP renders the cells resistant to Mb-induced oxidative stress (Figure 3, Table III). At least for the case of *SOD*, gene inhibition was matched with decreased

Table III. Fold-change in antioxidant and pro-inflammatory gene expression.

Gene- fold change (SD)	Treatment				
	Control	Mb (50 μM)	Mb (50 μM)+ *t*-BP (10 μM)	Mb (50 μM)+ *t*-BP (50 μM)	Mb (50 μM)+ *t*-BP (100 μM)
HO1	1.00 (0.0)	2.65 (0.2)*	2.05 (0.2)*	1.62 (0.6)#	1.83 (0.3)*#
SOD2	1.00 (0.0)	1.74 (0.3)*	1.68 (0.3)*	0.77 (0.1)#	0.98 (0.1)#
TNF-*a*	1.00 (0.0)	5.86 (0.6)*	3.39 (0.9)*#	1.67 (0.5)#	3.39 (1.2)*#
VCAM	1.00 (0.0)	1.90 (0.4)*	1.36 (0.3)#	0.94 (0.0)#	1.12 (0.0)#
NFκB	1.00 (0.4)	1.77 (1.7)	1.28 (0.7)	0.69 (0.5)	0.83 (0.7)
ICAM	1.00 (0.2)	1.58 (1.2)	1.23 (0.7)	1.00 (0.5)	1.08 (0.3)

*Significantly different vs control; $p < 0.05$.
#Significantly different vs Mb-treated group; $p < 0.05$.

total *SOD* activity (Figure 4). In addition, *t*-BP pre-treatment significantly enhanced monolayer permeability in the presence of extracellular Mb at doses ≥ 50 μM (Figure 5B), indicative of sustained tight junction function. In general, supplementation with *t*-BP restored receptor-mediated transport of labelled transferrin (Figures 6D–F and 7). Although endocytosis was not completely restored in *t*-BP-pre-treated cells exposed to 100 μM Mb (Figures 6F and 7), the extent of transferrin endocytosis remained significantly greater than that measured in the absence of *t*-BP (cf. Figures 6C and F).

Discussion

Herein we have identified key biochemical and molecular changes in cultured kidney epithelial cells exposed to a challenge of extracellular Mb as a model for burns-induced myoglobinuria. Cultured kidney epithelial cells responded to a relatively mild Mb-insult by increasing a range of antioxidant response elements to combat oxidative stress. Genes encoding early response antioxidants (*SOD*-1/2, *HO*-1) and pro-inflammatory (*TNFa* and *VCAM*) elements and the TSH redox status markedly increased and decreased, respectively, yet cell viability remained largely unaffected when assessed 24 h post-Mb insult. In parallel with enhanced oxidative stress, intracellular ATP was diminished significantly and both monolayer permissiveness and the endocytosis of labelled transferrin were inhibited. In contrast, supplementation of the kidney epithelial cells with ≥50 μM of the synthetic antioxidant *t*-BP (corresponding to pharmacologically achievable concentrations in rabbits [23] and mice [24]) prior to challenge with Mb inhibited oxidative stress, preserved the pool of intracellular ATP, dampened the endogenous antioxidant and proinflammatory gene responses and reversed the loss of monolayer permissiveness and receptor-mediated endocytosis. These data suggest that *t*-BP has some potential as a renal-protective agent at least when administered before the onset of experimental myoglobinuria. If Mb-induced oxidative stress were to play a role in promoting renal dysfunction in patients with severe burns, then supplementation with superior phenolic antioxidants of this type may provide a useful adjunctive therapy to preserve renal function.

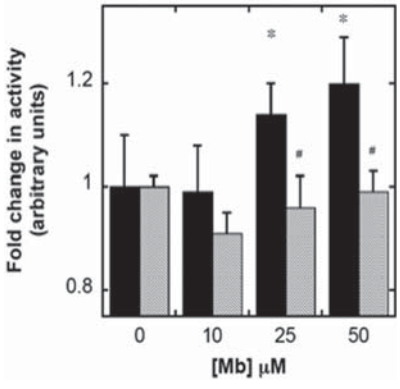

Figure 4. Effects of Mb treatment on total SOD activity in cultured kidney epithelial cells. Confluent MDCK II cells were treated in the absence (*control*) or presence of 100 μM *t*-BP and exposed to Mb (*dose shown*). After 24 h, control (*black bars*) or *t*-BP pre-treated cells (*hatched bars*) were harvested and lysed and total SOD activity assessed. Data represent mean ± SD from $n = 5$ experiments. *Significantly different to the control; $p < 0.05$. #Significantly different to the corresponding Mb-treated group; $p < 0.05$.

It is increasingly understood that oxidative stress can play a role in modulating cellular function in a range of cell types [36]. Receptor-mediated endocytosis and passive transport play a crucial role in membranous transport function within kidney tubules. The systematic decrease in transferrin internalisation and monolayer permissiveness as a function of Mb concentration highlights the potential for low Mb concentrations to promote inefficient kidney filtration, which is a hallmark of ARF. It follows that the demonstrable oxidative stress measured in the cultured epithelial cells upon exposure to Mb may be responsible for decreasing receptor-mediated endocytosis and passive transport. Consistent with this idea, transferrin receptors at the cell surface are sensitive to oxidative stress, and this likely involves thiol oxida-

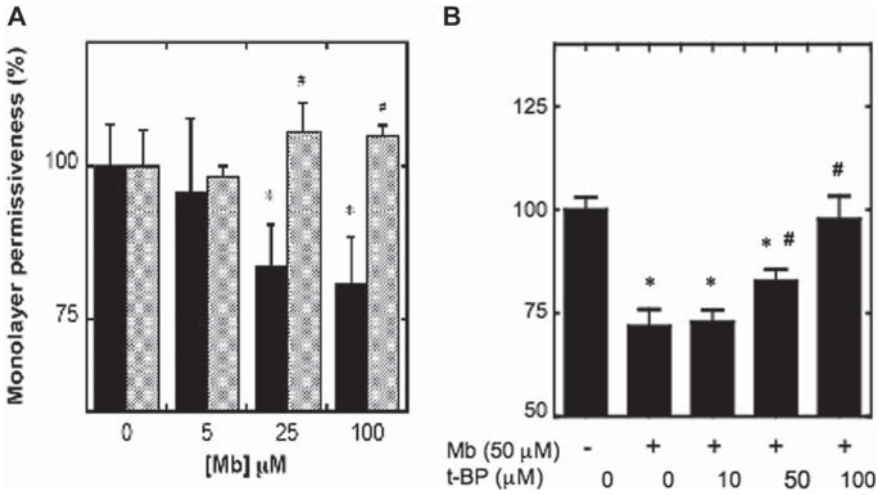

Figure 5. Monolayer permissiveness decreases in MDCK II cells after exposure to extracellular Mb. (A) Non-specific [^{3}H]-inulin transport in the absence (*black bars*) or presence of 100 μM *t*-BP (*hatched bars*). (B) Monolayers permissiveness improves in the presence of [*t*-BP] ≥ 50 μM but not 10 μM *t*-BP. Data represents mean ± SD from $n = 4$ experiments. *Significantly different to control; $p < 0.05$. #Significantly different to the Mb-treated group in the absence of *t*-BP; $p < 0.05$.

tion in scaffolding proteins within the cell membrane [35,37]. In addition, the passive flow of ions/solutes between adjacent epithelial cells can be modulated by oxidative stress, potentially via swelling of tight junctions [38], hence explaining the decrease in monolayer permissiveness determined here. Importantly, supplementation of the cultured epithelial cells with the synthetic antioxidant *t*-BP prior to Mb-treatment largely rescues receptor-mediated endocytosis and maintains tight junction integrity. This protection, afforded through bolstering cellular antioxidant capacity, is further evidence to support the notion that accumulating Mb likely disrupts kidney tubule function through a mechanism involving enhanced oxidative stress.

Impaired endothelial function may also play a role in damaging renal tissues, which are acutely susceptible to impaired blood flow [39]. For example, the inappropriate and sustained endothelial activation can compromise peritubular flow and promote renal dysfunction [40]. As a result the endothelium has become a target for the development of renal protective agents [41]. Central to normal vascular function is •NO bioavailability [42]. Extracellular Mb is implicated in modulating •NO levels through a range of chemical interactions (outlined in the Introduction section). In addition to these mechanisms of •NO-regulation, extracellular Mb can enhance oxidative stress through its ability to react with low-molecular weight peroxides, converting them to a mixture of the more potent two- and one-electron oxidants [12,16]. Exposure of endothelial cells or an intact endothelium to oxidants increases oxidative stress and results in the accumulation of $O_2^{\bullet-}$ that may be produced by multiple cellular sources [43]. Therefore, the ability of *t*-BP to inhibit the formation of Mb-derived oxidants through a mechanism of oxidant scavenging is likely to indirectly protect the vascular endothelium and potentially assist in maintaining vascular function within renal tissues.

Endogenous antioxidants are central to the protective mechanism against an oxidative challenge. Proteins such as *SOD* and the inducible *HO* are important early response elements in cellular defense [44]. Underpinning cell survival is an increased antioxidant capacity that enhances the intrinsic ability to dismutate $O_2^{\bullet-}$, opens pathways to regulate toxic peroxides and/or generate metabolites with antioxidant activity. As an example of the latter, haem metabolism generates the antioxidant bilirubin and simultaneously releases CO that readily activates soluble guanylyl cyclase to yield guanosine-3',5'-cyclic monophosphate [45]. Bilirubin and guanosine-3',5'-cyclic monophosphate are implicated in protecting renal cells from exogenous challenge [46,47]. Therefore, in response to Mb-insult, induction of *HO-1* and *SOD-1/2* enhances cellular antioxidant capacity to counter oxidative stress. Despite this endogenous response, extracellular Mb was able to stimulate epithelial cell dysfunction through inhibiting Fe metabolism and non-specific permissiveness, although this was not related to changes in cell viability.

The extent of Mb-induced epithelial cell dysfunction may be due to an inadequacy of the endogenous antioxidants and/or mechanisms to protect the cells from damage. Such damage may potentially lead to an inflammatory response by inducing pro-inflammatory cytokines and adhesion molecules [48]. The activation of the redox sensitive transcription factor NF-κB by shifts in the cellular microenvironments induces the production of pro-inflammatory stimuli, which lasts as long as the oxidative stress is sustained [49]. Studies in mouse models have shown that NF-κB production peaks at 4 h after stimulation and the

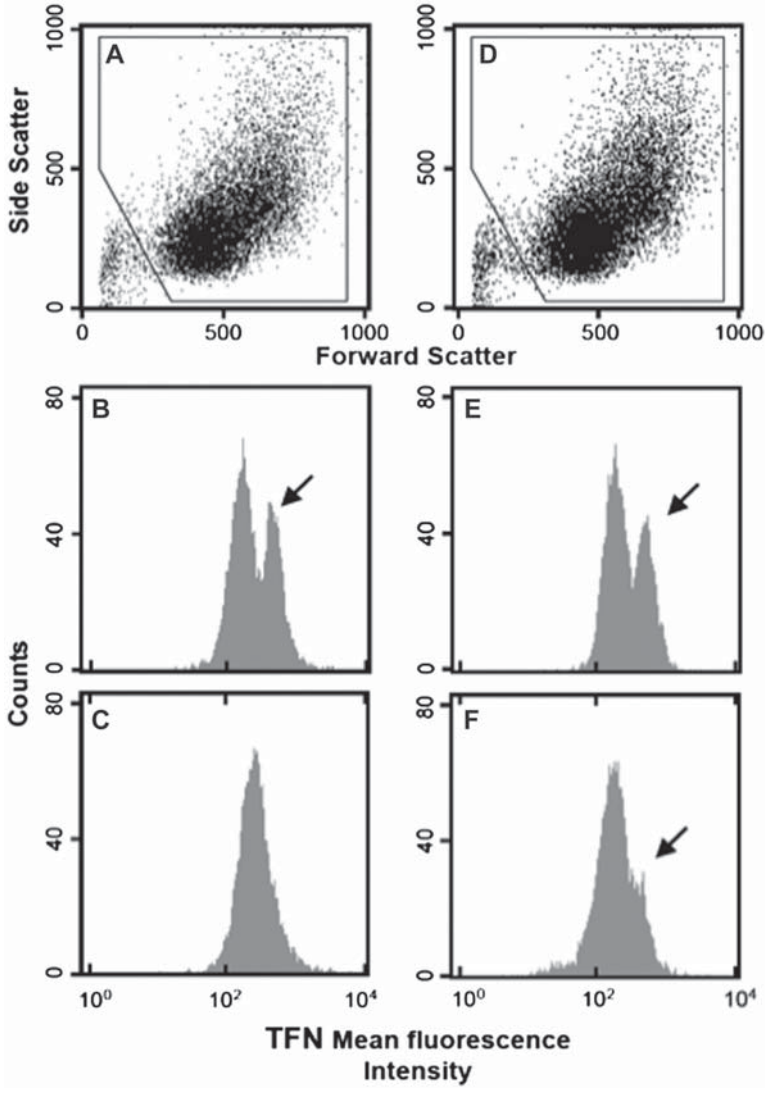

Figure 6. Endocytosis of labelled transferrin (TFN) in MDCK II cells. Mb-treated cells were incubated with TFN (125 μg/500 μL) for 10 min at 37°C prior to analysis. Panels (A–C) and (D–F) show data obtained in the absence and presence of 100 μM *t*-BP, respectively. Representative scatter plots of untreated controls in the (A) absence or (B) presence of *t*-BP are shown. Representative histograms of the respective controls in the absence (B) or presence (E) of *t*-BP but without Mb added, and samples treated with 100 μM Mb without (C) or with (F) added *t*-BP. Arrow indicates declining peak response.

expression then rapidly declines [50]. Downstream genes, including, but not restricted to TNFα, VCAM and ICAM (monitored here) once activated, engage in recruiting macrophages and lymphocytes, leading to a sustained inflammatory response, as shown in human proximal tubular epithelial cells [51]. Our data indicate that endogenous antioxidant response elements cannot overcome the Mb-challenge and that supplementation with the polyphenol *t*-BP potently inhibits early markers of renal cell inflammation.

The notion that dietary (phenolic) antioxidants can be renal-protective has significant merit with some [52–54], though not all [55–57], studies reporting improved renal function upon antioxidant supplementation. Our data demonstrate that the polyphenol *t*-BP protects kidney epithelial cells primarily through inhibiting Mb-induced oxidative stress, thereby modulating the signal for a cascade of events leading to epithelial cell dysfunction. A direct comparison of the potential renal-protective activity of phenols such as resveratrol or vitamin E with that of *t*-BP has not been assessed here or elsewhere. However, it is worth noting that *t*-BP was strategically designed from a structure function analysis of over 60 antioxidant compounds [58] including natural and synthetic (poly)phenols. Comparatively, *t*-BP is a superior radical scavenging agent that can synergise with vitamin E to enhance antioxidant activity (refer to Table II). Therefore, it is likely that *t*-BP is a suitable candidate for interventional studies using an animal model of myoglobinuria that mimics severe burns. A better understanding of the role for Mb in promoting both oxidative stress and dysfunction in renal tissues may

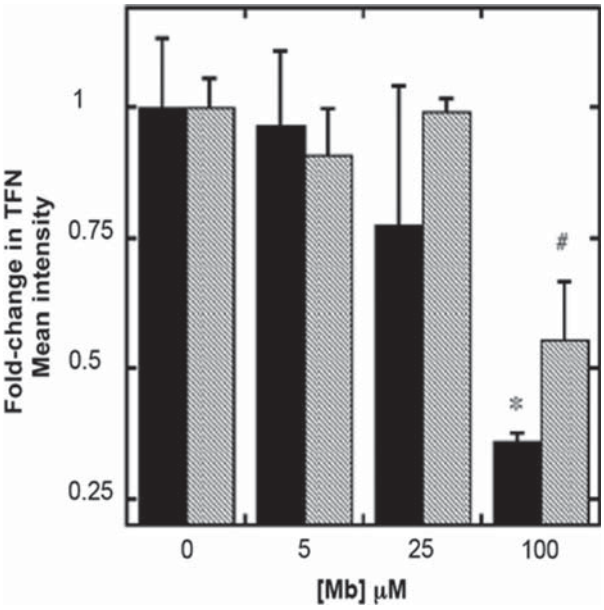

Figure 7. Inhibition of endocytosis by added Mb is reversed by pre-treatment of cells with *t*-BP. Raw data was obtained as described in the legend to Figure 6 and re-expressed as mean data for the various treatment groups. Data represent mean ± SD from $n = 4$ experiments. *Significantly different to the control; $p < 0.05$. #Significantly different to the corresponding Mb-treated group; $p < 0.05$.

lead to the development of (antioxidant-based) therapies that benefit burns patients.

Declaration of interest: We thank the support from the Australian Research Council (Fellowship DP0343325 and Discovery DP0878559 Grants to PKW). The authors report no conflicts of interest. The authors alone are responsible for the content and writing of the paper.

References

[1] Kim GH, Oh KH, Yoon JW, Koo JW, Kim HJ, Chae DW, Noh JW, Kim JH, Park YK. Impact of burn size and initial serum albumin level on acute renal failure occurring in major burn. Am J Nephrol 2003;23:55–60.

[2] Mustonen KM, Vuola J. Acute renal failure in intensive care burn patients (ARF in burn patients). J Burn Care Res 2008;29:227–237.

[3] Holm C, Horbrand F, von Donnersmarck GH, Muhlbauer W. Acute renal failure in severely burned patients. Burns 1999; 25:171–178.

[4] Vertel RM, Knochel JP. Nonoliguric acute renal failure. Jama 1967;200:598–602.

[5] Davies DM, Pusey CD, Rainford DJ, Brown JM, Bennett JP. Acute renal failure in burns. Scand J Plast Reconstr Surg 1979;13:189–192.

[6] Chrysopoulo MT, Jeschke MG, Dziewulski P, Barrow RE, Herndon DN. Acute renal dysfunction in severely burned adults. J Trauma 1999;46:141–144.

[7] Moore KP, Holt SG, Patel RP, Svistunenko DA, Zackert W, Goodier D, Reeder BJ, Clozel M, Anand R, Cooper CE, Morrow JD, Wilson MT, Darley-Usmar V, Roberts LJ 2nd. A causative role for redox cycling of myoglobin and its inhibition by alkalinization in the pathogenesis and treatment of rhabdomyolysis-induced renal failure. J Biol Chem 1998;273,31731–31737.

[8] Reeder BJ, Svistunenko DA, Cooper CE, Wilson MT. The radical and redox chemistry of myoglobin and hemoglobin: from *in vitro* studies to human pathology. Antioxid Redox Signal 2004;6:954–966.

[9] Reeder BJ, Sharpe MA, Kay AD, Kerr M, Moore K, Wilson MT. Toxicity of myoglobin and haemoglobin: oxidative stress in patients with rhabdomyolysis and subarachnoid haemorrhage. Biochem Soc Trans 2002;30:745–748.

[10] Vetterlein F, Hoffmann F, Pedina J, Neckel M, Schmidt G. Disturbances in renal microcirculation induced by myoglobin and hemorrhagic hypotension in anesthetized rat. Am J Physiol 1995;268:839–846.

[11] Zager RA. Rhabdomyolysis and myohemoglobinuric acute renal failure. Kidney Int 1996;49:314–326.

[12] Witting PK, Mauk AG. Reaction of human myoglobin and H_2O_2. Electron transfer between tyrosine 103 phenoxyl radical and cysteine 110 yields a protein-thiyl radical. J Biol Chem 2001;276:16540–16547.

[13] Holt S, Reeder B, Wilson M, Harvey S, Morrow JD, Roberts LJ, 2nd, Moore K. Increased lipid peroxidation in patients with rhabdomyolysis. Lancet 1999;353:1241.

[14] Rayner BS, Wu BJ, Raftery M, Stocker R, Witting PK. Human S-nitroso oxymyoglobin is a store of vasoactive nitric oxide. J Biol Chem 2005;280:9985–9993.

[15] Andriambeloson E, Witting PK. Chemical regulation of nitric oxide: a role for intracellular myoglobin? Redox Rep 2002;7: 131–136.

[16] Rayner BS, Stocker R, Lay PA, Witting PK. Regio- and stereochemical oxidation of linoleic acid by human myoglobin and hydrogen peroxide: Tyr(103) affects rate and product distribution. Biochem J 2004;381:365–372.

[17] D'Agnillo F, Alayash AI. A role for the myoglobin redox cycle in the induction of endothelial cell apoptosis. Free Radic Biol Med 2002;33:1153–1164.

[18] Reeder BJ, Svistunenko DA, Sharpe MA, Wilson MT. Characteristics and mechanism of formation of peroxide-induced heme to protein cross-linking in myoglobin. Biochemistry 2002;41:367–375.

[19] Parry SN, Ellis N, Li Z, Maitz P, Witting PK. Myoglobin induces oxidative stress and decreases endocytosis and monolayer permissiveness in cultured kidney epithelial cells without affecting viability. Kidney Blood Press Res 2008; 31:16–28.

[20] Himmelfarb J, McMonagle E, Freedman S, Klenzak J, McMenamin E, Le P, Pupim LB, Ikizler TA, The PICARD Group. Oxidative stress is increased in Critically Ill Patients with Acute Renal Failure. J Am Soc Nephrol 2004;15:2449–2456.

[21] Vazhiri ND. Causal link between oxidative stress, inflammation, and hypertension. IJKD 2008;2:1–10.

[22] Kim SH, Chang JW, Kim SB, Park SK, Park JS, Lee SK. Myoglobin induces vascular cell adhesion molecule-1 expression through c-Src kinase-activator protein-1/nuclear factor-kappaB pathways. Nephron Exp Nephrol 2009;114:e48–e60.

[23] Witting P, Pettersson K, Ostlund-Lindqvist AM, Westerlund C, Wagberg M, Stocker R. Dissociation of atherogenesis from aortic accumulation of lipid hydro(pero)xides in Watanabe heritable hyperlipidemic rabbits. J Clin Invest 1999;104: 213–220.

[24] Witting PK, Pettersson K, Ostlund-Lindqvist AM, Westerlund C, Eriksson AW, Stocker R. Inhibition by a coantioxidant of aortic lipoprotein lipid peroxidation and atherosclerosis in apolipoprotein E and low density lipoprotein receptor gene double knockout mice. Faseb J 1999;13:667–675.

[25] Rayner BS, Duong TT, Myers SJ, Witting PK. Protective effect of a synthetic anti-oxidant on neuronal cell apoptosis

resulting from experimental hypoxia re-oxygenation injury. J Neurochem 2006;97:211–221.
[26] Koopman G, Reutelingsperger CP, Kuijten GA, Keehnen RM, Pals ST, van Oers M. Annexin V for flow cytometric detection of phosphatidylserine expression on B cells undergoing apoptosis. Blood 1994;84:1415–1420.
[27] Duong TT, Antao S, Ellis NA, Myers SJ, Witting PK. Supplementation with a synthetic polyphenol limits oxidative stress and enhances neuronal cell viability in response to hypoxia-re-oxygenation injury. Brain Res 2008;1219:8–18.
[28] Ahmed H, Schott EJ, Gauthier JD, Vasta GR. Superoxide dismutases from the oyster parasite Perkinsus marinus: purification, biochemical characterization, and development of a plate microassay for activity. Anal Biochem 2003;318: 132–141.
[29] Apodaca G, Bomsel M, Lindstedt R, Engel J, Frank D, Mostov KE, Wiener-Kronish J. Characterization of Pseudomonas aeruginosa-induced MDCK cell injury: glycosylation-defective host cells are resistant to bacterial killing. Infect Immun 1995;63:1541–1551.
[30] Leo A, Hansch C, Elkins D. Partition coefficients and their uses. Chem Rev 1971;71:525–616.
[31] Buettner GR. The pecking order of free radicals and antioxidants: lipid peroxidation, alpha-tocopherol, and ascorbate. Arch Biochem Biophys 1993;300:535–543.
[32] Hack B, Witting PK, Rayner BS, Stocker R, Headrick JP. Oxidant stress and damage in post-ischemic mouse hearts: effects of adenosine. Mol Cell Biochem 2006;287:165–175.
[33] Von Bonsdorff CH, Fuller SD, Simons K. Apical and basolateral endocytosis in Madin-Darby canine kidney (MDCK) cells grown on nitrocellulose filters. Embo J 1985;4:2781–2792.
[34] Hurley BP, Jacewicz M, Thorpe CM, Lincicome LL, King AJ, Keusch GT, Acheson DW. Shiga toxins 1 and 2 translocate differently across polarized intestinal epithelial cells. Infect Immun 1999;67:6670–6677.
[35] Malorni W, Testa U, Rainaldi G, Tritarelli E, Peschle C. Oxidative stress leads to a rapid alteration of transferrin receptor intravesicular trafficking. Exp Cell Res 1998;241:102–116.
[36] Halliwell B. Antioxidant defence mechanisms: from the beginning to the end (of the beginning). Free Rad Res 1999;31:261–272.
[37] Malorni W, Iosi F, Santini MT, Testa U. Menadione-induced oxidative stress leads to a rapid down-modulation of transferrin receptor recycling. J Cell Sci 1993;106:309–318.
[38] Cereijido M, Valdes J, Shoshani L, Contreras RG. Role of tight junctions in establishing and maintaining cell polarity. Ann Rev Physiol 1998;60:161–177.
[39] Alcazar JM, Caramelo CA, Alegre ER, Abad J. Ischaemic renal injury. Curr Opin Nephrol Hypertens 1997;6:157–165.
[40] Rabelink TJ, Wijewickrama DC, de Koning EJ. Peritubular endothelium: the Achilles heel of the kidney? Kidney Int 2007;72:926–930.
[41] Zoccali C. The endothelium as a target in renal diseases. J Nephrol 2007;20:39–44.
[42] Thomas SR, Witting PK, Drummond GR. Redox control of endothelial function and dysfunction: molecular mechanisms and therapeutic opportunities. Antioxid Redox Signal. 2008; 10:1713–1765.
[43] Witting PK, Rayner BS, Wu BJ, Ellis NA, Stocker R. Hydrogen peroxide promotes endothelial dysfunction by stimulating multiple sources of superoxide anion radical production and decreasing nitric oxide bioavailability. Cell Physiol Biochem 2007;20:255–268.
[44] Witting P, Stocker R. Ascorbic acid as an antioxidant in atherosclerosis. In: May J, Hasard A, Smirnoff N, editors. Vitamin C: Its functions and biochemistry in animals and plants. Oxford: Bios Scientific Publishers; 2004. p261–290.
[45] Friebe A, Schultz G, Koesling D. Sensitizing soluble guanylyl cyclase to become a highly CO-sensitive enzyme. Embo J 1996;15:6863–6868.
[46] Kirkby KA, Adin CA. Products of heme oxygenase and their potential therapeutic applications. Am J Physiol Renal Physiol 2006;290:563–571.
[47] Gonzalez-Michaca L, Farrugia G, Croatt AJ, Alam J, Nath KA. Heme: a determinant of life and death in renal tubular epithelial cells. Am J Physiol Renal Physiol 2004; 286:370–377.
[48] Tian N, Moore RS, Braddy S, Rose RA, Gu JW, Hughson MD, Manning RD Jr. Interactions between oxidative stress and inflammation in salt-sensitive hypertension. Am J Physiol Heart Circ Physiol 2007;293:H3388–H3395.
[49] Rodríguez-Iturbe B, Vaziri ND, Herrera-Acosta J, Johnson RJ. Oxidative stress, renal infiltration of immune cells, and salt-sensitive hypertension: all for one and one for all. Am J Physiol Renal Physiol 2004;286:F606–F616.
[50] Saban MR, Hellmich H, Nguyen N, Winston J, Hammond TG, Saban R. Time course of LPS-induced gene expression in a mouse model of genitourinary inflammation. Physiol Genomics 2001;5:147–160.
[51] Ho AWY, Wong CK, Lam CWK. Tumor necrosis factor-a up-regulates the expression of CCL2 and adhesion molecules of human proximal tubular epithelial cells through MAPK signaling pathways. Immunobiology 2008;213:533–544.
[52] Hisamura F, Kojima-Yuasa A, Huang X, Kennedy DO, Matsui-Yuasa I. Synergistic effect of green tea polyphenols on their protection against FK506-induced cytotoxicity in renal cells. Am J Chin Med 2008;36:615-624.
[53] Karhumaki P, Tiitinen SL, Turpeinen H, Parkkinen J. Inhibition of ERK1/2 activation by phenolic antioxidants protects kidney tubular cells during cold storage. Transplantation 2007;83:948–953.
[54] Chander V, Chopra K. Protective effect of resveratrol, a polyphenolic phytoalexin on glycerol-induced acute renal failure in rat kidney. Ren Fail 2006;28:161–169.
[55] Fernández-Fúnez A, Polo FJ, Broseta L, Valer J, Zafrilla L. Effects of N-acetylcysteine on myoglobinuric-acute renal failure in rats. Ren Fail 2002;24:725–733.
[56] Vlahović P, Cvetković T, Savić V, Stefanović V. Dietary curcumin does not protect kidney in glycerol-induced acute renal failure. Food Chem Toxicol 2007;45:1777–1782.
[57] Brown CV, Rhee P, Chan L, Evans K, Demetriades D, Velmahos GC. Preventing renal failure in patients with rhabdomyolysis: do bicarbonate and mannitol make a difference? J Trauma 2004;56:1191–1196.
[58] Witting PK, Westerlund C, Stocker R. A rapid and simple screening test for potential inhibitors of tocopherol-mediated peroxidation of LDL lipids. J Lipid Res 1996;37:853–867.
[59] Wu BJ, Kathir K, Witting PK, Beck K, Choy K, Li C, Croft KD, Mori TA, Tanous D, Adams MR, Lau AK, Stocker R. Antioxidants protect from atherosclerosis by a heme oxygenase-1 pathway that is independent of free radical scavenging. J Exp Med 2006;203:1117–1127.

This paper was first published online on Early Online on 20 May 2010.